Journal of Applied Fluid Mechanics , Vol. 9, No. 1, pp. 11-17, 2016.
Available online at www.jafmonline.net, ISSN 1735-3572, EISSN 1735-3645.
DOI: 10.18869/acadpub.jafm.68.224.23964

Magnetohydrodynamic Boundary Layer Slip Flow and Heat Transfer of Power Law Fluid over a Flat Plate

J. Hirschhorn[1], M. Madsen[1], A. Mastroberardino[2†] and J. I. Siddique[1]

[1] *Penn State University, York Campus, York, Pennsylvania 17403-3326, USA*
[2] *Penn State Erie, The Behrend College, Erie, Pennsylvania 16563-0203, USA*

†*Corresponding Author Email*: *axm62@psu.edu*

(Received August 2, 2014; accepted October 5, 2014)

ABSTRACT

In this paper, we consider the magnetohydrodynamic (MHD) boundary layer flow and heat transfer of power law fluid over a flat plate with slip boundary conditions. We use a similarity transformation to convert the governing nonlinear partial differential equations into a system of ordinary differential equations and solve the resulting system numerically using MATLAB's boundary value solver, bvp4c, and the shooting method. We present velocity and temperature profiles within the boundary layer and demonstrate the effect of changing the magnetic parameter, Prandtl number, and slip parameters.

Keywords: Magnetohydrodynamic flow; Nonlinear boundary value problem; Slip flow; Non-Newtonian fluid.

1. INTRODUCTION

The layer of fluid that flows directly adjacent to its bounding surface is called the boundary layer. The boundary layer is an extremely important concept in fluid mechanics and has been studied extensively for decades. Fluid motion in the boundary layer is influenced by a number of factors including fluid viscosity, bounding surface characteristics, and external forces, to name a few. Models are being continuously developed and refined to demonstrate the interaction between these factors and their effect on fluid flow in the boundary layer.

Some refinements of the boundary layer model have focused on forced convection of viscous fluids past their bounding surfaces, thus incorporating an analysis of heat transfer, such as the study of vertical flat plates imbedded in porous media by Pop and Takhar (Pop and Takhar 1983). The inclusion of heat transfer in studies of fluid flow has greatly expanded the applicability of modeling to the aviation, petroleum refinement, and food processing industries. These thermodynamic models were further extended by the work of Damseh *et al.* (Damseh, Duwairi, and Al-Odat 2006) who, among others, demonstrated the effect of magnetic fields on the flow of electrically conductive fluids. This analysis of MHD fluids became vitally important in the operation of pumps, turbines, and bearings. Martin and Boyd (Martin and Boyd 2006) and Bhattacharyya *et al.* (Bhattacharyya, Mukhopadhyay, and Layek 2011) incorporated velocity and thermal slip conditions in their studies of laminar flow across flat plates to further refine our understanding of boundary layer flow.

Many models consider only Newtonian fluids, for which strain rate is linearly related to applied shear stress. As non-Newtonian fluids—classified as either pseudoplastic or dilatant—have become more common in industry, analysis of the boundary layer flow and heat transfer characteristics of these so-called power law fluids is now a priority. Dilatant fluids, or shear thickening fluids, are liquids in which viscosity increases as the applied stress increases, whereas pseudoplastics, or shear thinning fluids, are characterized by the opposite relationship between viscosity and applied stress. Two of the first studies that considered power law fluids were performed by Acrivos *et al.* (Acrivos, Shah, and Petersen 1960) and Schowalter (Schowalter 1960). Howell *et al.* (Howell, Jeng, and DeWitt 1997) provided a

notable extension of these works with a study of the flow of power law fluid over a continuously moving and stretching surface. Recent additions considering magnetohydrodynamic flow were given by Ghosh and Pop (Ghosh and Pop 2006), Mahapatra *et al.* (Mahapatra, Nandy, and Gupta 2009) and Reddy *et al.* (Reddy, Kishan, and Rajasekhar 2012).

In this article, we study MHD boundary layer flow of power law fluid over a flat plate. We consider a modified version of the slip model by Anderson in (Anderson 2002) by incorporating features of the thermal slip model presented by Bhattacharyya *et al.* (Bhattacharyya, Mukhopadhyay, and Layek 2011). The resulting system of equations is solved using MATLAB's boundary value solver, bvp4c, and by the shooting method. We demonstrate the agreement between the results obtained by these two methods by plotting a direct comparison. In this study, we seek to collect all of the factors mentioned above into a single, comprehensive model by incorporating MHD effects, velocity and thermal slip boundary conditions, and flow of a power law fluid. We present plots of the numerically computed solutions and discuss some of the interesting correlations observed between the various physical parameters.

2. MATHEMATICAL FORMULATION

To construct our model, we consider steady, laminar flow of an electrically conductive, viscous fluid. As depicted in Figure 1, we place this fluid in a two-dimensional environment over a flat plate and in the presence of a transverse magnetic field. We invoke conservation of mass, momentum balance, and conservation of energy to describe the fluid flow and heat transfer in the boundary layer using the equations (Howell, Jeng, and DeWitt 1997)

$$\frac{\partial u}{\partial x}+\frac{\partial u}{\partial y}=0, \tag{2..1}$$

$$u\frac{\partial u}{\partial x}+v\frac{\partial u}{\partial y}=\frac{1}{\rho}\frac{\partial \tau_{xy}}{\partial y}-\frac{\sigma B^2}{\rho}\left(u-U_\infty\right) \tag{2..2}$$

$$u\frac{\partial T}{\partial x}+v\frac{\partial T}{\partial y}=\frac{\kappa}{\rho c_p}\frac{\partial^2 T}{\partial y^2}, \tag{2..3}$$

where u is the component of velocity along the x-axis, v is the component of velocity along the y-axis, ρ is the fluid density, τ_{xy} is the shear stress, σ is the constant electrical conductivity of the fluid, B is the magnetic field strength, U_∞ is the free stream velocity, T is temperature, κ is the thermal conductivity, and c_p is the specific heat capacity of the fluid. Equations (2..1) - (2..3) are subject to the boundary conditions

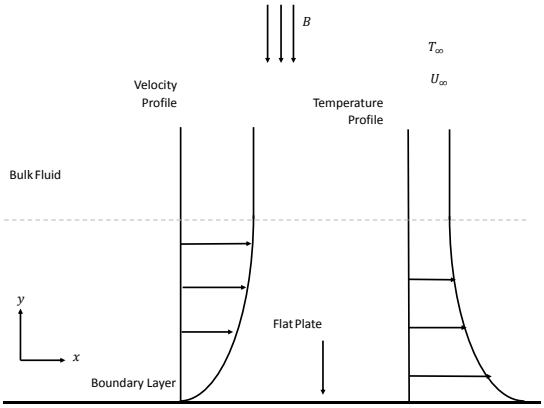

Fig. 1. Schematic diagram of MHD boundary layer flow over a flat plate.

$$u=L_1\left(\partial u/\partial y\right), \quad v=0 \quad at \quad y=0;$$
$$u\to U_\infty \quad as \quad y\to\infty, \tag{2..4}$$
$$T=T_w+D_1\left(\partial T/\partial y\right) \quad at \quad y=0;$$
$$T\to T_\infty \quad as \quad y\to\infty, \tag{2..5}$$

where $L_1=L\sqrt{Re_x}$ is the velocity slip factor with L being the initial value at the leading edge and $D_1=D\sqrt{Re_x}$ is the thermal slip factor with D being the initial value at the leading edge. Here, T_w is the temperature of the flat plate, T_∞ is the free stream temperature, and $Re_x=\frac{U_\infty^{2-n}x^n\rho}{K}$ is the local Reynolds number. We further define the shear stress as (Mahapatra, Nandy, and Gupta 2009)

$$\tau_{xy}=K\left|\frac{\partial u}{\partial y}\right|^{n-1}\frac{\partial u}{\partial y}, \tag{2..6}$$

where n is the power law index and K is the consistency coefficient. Note that K is a generalization of the dynamic viscosity μ, which would take its place in the Newtonian case when $n=1$.

We substitute equation (2..6) into equation (2..2) to obtain

$$u\frac{\partial u}{\partial x}+v\frac{\partial u}{\partial y}=\frac{K}{\rho}\frac{\partial}{\partial y}\left(\left|\frac{\partial u}{\partial y}\right|^{n-1}\frac{\partial u}{\partial y}\right)$$
$$-\frac{\sigma B^2}{\rho}\left(u-U_\infty\right). \tag{2..7}$$

Equations (2..1), (2..3), and (2..7) are then mapped into a planar geometry by introducing the stream function $\psi(x,y)$

$$u=\frac{\partial \psi}{\partial y}, \quad v=-\frac{\partial \psi}{\partial x}, \tag{2..8}$$

which identically satisfies equation (2..1) and transforms equations (2..7) and (2..3) into

$$\frac{\partial\psi}{\partial y}\frac{\partial^2\psi}{\partial x\partial y}-\frac{\partial\psi}{\partial x}\frac{\partial^2\psi}{\partial y^2}=\frac{K}{\rho}\frac{\partial}{\partial y}\left(\left|\frac{\partial^2\psi}{\partial y^2}\right|^{n-1}\frac{\partial^2\psi}{\partial y^2}\right)$$
$$-\frac{\sigma B^2}{\rho}\left(\frac{\partial\psi}{\partial y}-U_\infty\right), \qquad (2..9)$$
$$\frac{\partial\psi}{\partial y}\frac{\partial T}{\partial x}-\frac{\partial\psi}{\partial x}\frac{\partial T}{\partial y}=\frac{\kappa}{\rho c_p}\frac{\partial^2 T}{\partial y^2}. \qquad (2..10)$$

Boundary condition (2..4) is likewise transformed into

$$\frac{\partial\psi}{\partial y}=L_1\frac{\partial^2\psi}{\partial y^2},\quad \frac{\partial\psi}{\partial x}=0\quad at\quad y=0;$$
$$\frac{\partial\psi}{\partial y}\to U_\infty\quad as\quad y\to\infty. \qquad (2..11)$$

3. METHOD OF SOLUTION

In order to obtain solutions, we apply similarity transformations to equations (2..5) and (2..9) - (2..11) to transform them into a non-linear boundary value problem involving a system of ordinary differential equations. Specifically, we introduce the dimensionless similarity variables used by Reddy *et al.* (Reddy, Kishan, and Rajasekhar 2012) and defined as

$$\psi=\ell U_\infty\left(\frac{\frac{x}{\ell}}{Re}\right)^{\frac{1}{n+1}}f(\eta), \qquad (3..12)$$
$$T=T_\infty+(T_w-T_\infty)\,\theta(\eta), \qquad (3..13)$$

where ℓ is the characteristic length and *Re* is the generalized Reynolds number. We further define the similarity variable η and *Re* as

$$\eta=\left(\frac{Re}{\frac{x}{\ell}}\right)^{\frac{1}{n+1}}\frac{y}{\ell}, \qquad (3..14)$$
$$Re=\frac{\rho U_\infty^{2-n}\ell^n}{K}. \qquad (3..15)$$

Application of the similarity transformations to equations (2..9) and (2..10) gives

$$n|f''|^{n-1}f'''+\frac{1}{n+1}ff''-M(f'-1)=0, \qquad (3..16)$$
$$\theta''+\frac{1}{n+1}Prf\theta'=0, \qquad (3..17)$$

where *M* is the magnetic parameter and *Pr* is the Prantdl number, further defined as

$$M=\frac{\sigma B^2 x}{\rho U_\infty}, \qquad (3..18)$$
$$Pr=\left(\frac{U_\infty^3}{x}\right)^{\frac{n-1}{n+1}}\frac{c_p\rho}{\kappa}\left(\frac{K}{\rho}\right)^{\frac{2}{n+1}}. \qquad (3..19)$$

Boundary conditions (2..11) and (2..5) are transformed into

$$f(\eta)=0,\quad f'(\eta)=\delta f''(\eta)\quad at\quad \eta=0;$$
$$f'(\eta)\to 1\quad as\quad \eta\to\infty, \qquad (3..20)$$
$$\theta(\eta)=1+\beta\theta'(\eta)\quad at\quad \eta=0;$$
$$\theta(\eta)\to 0\quad as\quad \eta\to\infty, \qquad (3..21)$$

where δ is the velocity slip parameter and β is the temperature slip parameter, which are further defined as

$$\delta=L\frac{U_\infty\rho}{K}, \qquad (3..22)$$
$$\beta=D\frac{U_\infty\rho}{K}. \qquad (3..23)$$

We now employ the MATLAB function bvp4c, a numerical method designed to solve boundary value problems similar to the one considered here. To utilize this function, we convert equations (3..16) and (3..17) to the first order system

$$f'=p,\quad p'=q,$$
$$q'=\frac{-1}{n(n+1)}fq^{2-n}+\frac{M}{n}(p-1)q^{1-n}, \qquad (3..24)$$
$$\theta'=z,\quad z'=\frac{-1}{n+1}Prfz, \qquad (3..25)$$

along with the boundary conditions

$$f(\eta)=0,\quad p(\eta)=\delta q(\eta)\quad at\quad \eta=0;$$
$$p(\eta)\to 1\quad as\quad \eta\to\infty, \qquad (3..26)$$
$$\theta(\eta)=1+\beta z(\eta)\quad at\quad \eta=0;$$
$$\theta(\eta)\to 0\quad as\quad \eta\to\infty. \qquad (3..27)$$

The function bvp4c requires initial guesses for $q(\eta)$ and $z(\eta)$ at $\eta=0$, and through iterative comparison, we modify each guess until we arrive at an appropriate solution for our problem. Note that bvp4c uses these initial guesses to generate solutions using a collocation method. We verify the correctness of these solutions by comparing them with those obtained using the shooting method. We find the results to be in good agreement as shown in Figure 2.

4. RESULTS AND DISCUSSION

We illustrate the effect of varying the power law index *n*, the magnetic parameter *M*, the velocity slip parameter δ, the temperature slip parameter β, and the Prandtl number *Pr* on boundary layer velocity $f'(\eta)$ and temperature $\theta(\eta)$ profiles. We present plots that demonstrate the

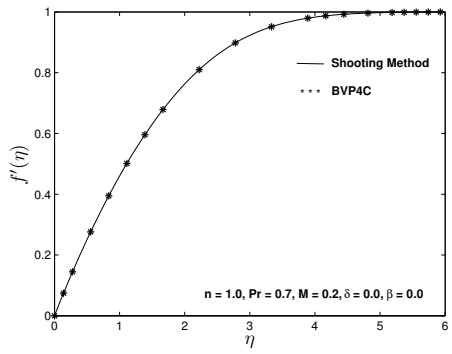

Fig. 2. Agreement between velocity $f'(\eta)$ profiles generated by the shooting method and bvp4c.

meaningful relationships between the parameters and provide a brief physical explanation for each situation.

The effect of varying the magnetic parameter M on fluid velocity $f'(\eta)$ is shown in Figure 3. By comparing two curves with the same power law index, it is clear that as the magnetic parameter increases, the velocity also inreases for a given distance from the flat plate. The presence of a transverse magnetic field thins the boundary layer by boosting fluid flow.

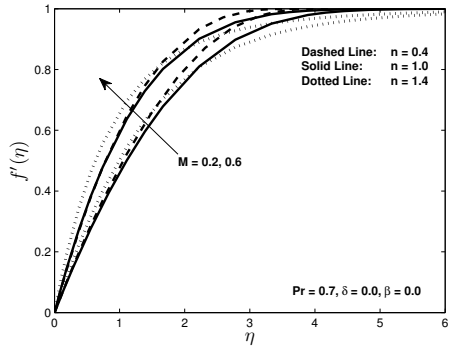

Fig. 3. Velocity $f'(\eta)$ profiles for various values of magnetic parameter M and power law index n.

However, interesting and less intuitive relationships arise when comparing curves with the same magnetic parameter M but different power law index n. Observe that shear-thinning fluids achieve the greatest fluid velocity $f'(\eta)$ as η increases from zero, followed by shear-thickening and Newtonian fluids. Shear-thinning fluid velocity rises faster than that of shear-thickening initially due to higher shear stress at that location. Shear-thinning fluids have a smaller effective viscosity than shear-thickening fluids at that point and thus achieve a higher strain rate and velocity. The velocity of shear-thinning fluids later decreases below that of shear-thickening fluids, and soon below that of Newtonian fluids. This trend is observed to be the opposite of the previous process. As shear stress decreases, the effective viscosity decreases for shear-thickening fluids and increases for shear-thinning fluids. The strain rate and velocity of shear-thickening fluids therefore increases.

Varying the magnetic parameter M also affects fluid temperature $\theta(\eta)$ as show in Figure 4. As the magnetic parameter M increases, the temperature of a power law fluid decreases for a given distance from the flat plate. This is because the transverse magnetic field boosts fluid flow, enhancing heat transfer to the fluid. It is important to note that temperature is dependent on velocity in situations where heat transfer is accomplished by convection, as this principle will also be important for following discussions.

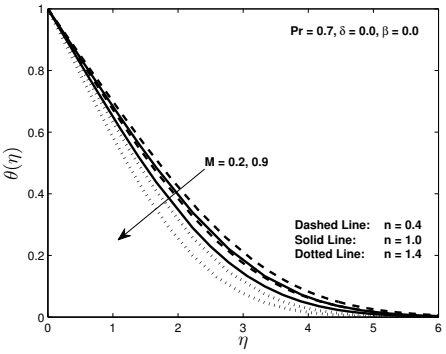

Fig. 4. Temperature $\theta(\eta)$ profiles for various values of magnetic parameter M and power law index n.

The effect of varying the velocity slip parameter δ on fluid velocity $f'(\eta)$ is shown in Figure 4. As the velocity slip parameter increases, the fluid velocity also increases for a given distance from the flat plate. As expected the thickness of the boundary layer decreases due to the positive value of fluid velocity at the surface of the flat plate.

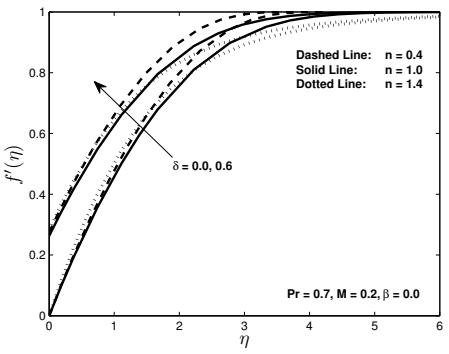

Fig. 5. Velocity $f'(\eta)$ profiles for various values of velocity slip parameter δ and power law index n.

Values of the skin friction coefficient $f''(0)$ are shown in Table 1 for various parameter values. Observe that shear-thinning fluids have the highest value of the skin friction coefficient followed by Newtonian and shear-thickening fluids when all other parameters are held constant. This is consistent with the higher rate of shear-thinning fluid velocity $f'(\eta)$ increase observed at the surface of the flat plate. The skin friction coefficient increases for a power law fluid as the magnetic parameter M is increased. Conversely, increasing the velocity slip parameter δ decreases the value of the skin friction coefficient. Note that as the velocity slip parameter approaches an infinite slip condition, the fluid velocity at the flat plate approaches free stream velocity, and the skin friction coefficient approaches zero. For these reasons, it is clear that an increase in the skin friction coefficient corresponds to a thinning of the velocity boundary layer.

Table 1. Values of the skin friction coefficient $f''(0)$.

n	M	δ	$f''(0)$
0.4	0.6	0.3	0.82269
1			0.68047
1.4			0.67638
1.4	0.2	0.3	0.55685
	0.6		0.67638
	1		0.78586
1.4	0.6	0	0.80059
		0.3	0.67638
		0.6	0.58017

Because of its dependency on fluid velocity $f'(\eta)$, fluid temperature $\theta(\eta)$ also varies with the velocity slip parameter δ as shown in Figure 5. As the velocity slip parameter increases, the temperature of a power law fluid decreases for a given distance from the flat plate. This is because the positive value of fluid velocity at the flat plate enhances heat transfer to the fluid.

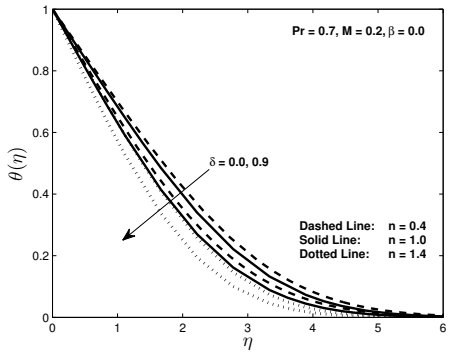

Fig. 6. Temperature $\theta(\eta)$ profiles for various values of velocity slip parameter δ and power law index n.

The effect of varying the temperature slip parameter β is shown in Figure 7. As the temperature slip parameter increases, the temperature $\theta(\eta)$ of a power law fluid decreases for a given distance from the flat plate. The thickness of the thermal boundary layer decreases due to the fluid at the surface of the flat plate having a temperature lower than that of the flat plate.

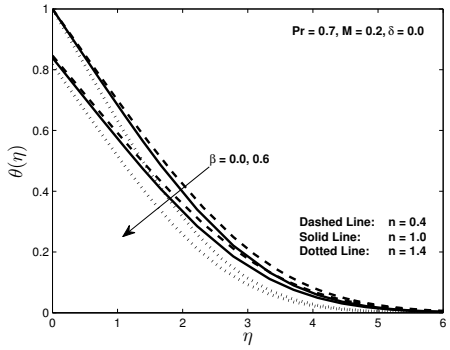

Fig. 7. Temperature $\theta(\eta)$ profiles for various values of temperature slip parameter β and power law index n.

The effect of varying the Prandtl number Pr, a ratio between momentum and thermal diffusivity, is shown in Figure 8. As the Prandtl number increases, the temperature $\theta(\eta)$ of a power law fluid decreases for a given distance from the flat plate. In general, it can be observed that the thermal boundary layer is thinner for fluids that transfer heat more effectively via convection than conduction.

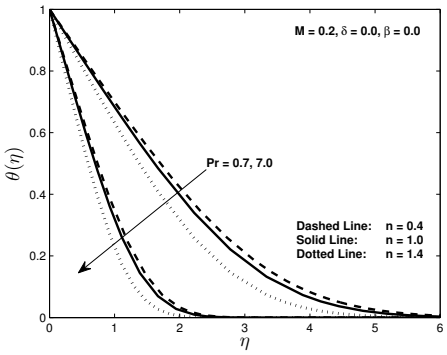

Fig. 8. Temperature $\theta(\eta)$ profiles for various values of Prandtl number *Pr* and power law index *n*.

Table 2. Values of the Nusselt number $-\theta'(0)$.

n	*M*	*Pr*	δ	β	$-\theta'(0)$
0.4	0.6	0.7	0.3	0.3	0.39319
1					0.33497
1.4					0.31484
1.4	0.2	0.7	0.3	0.3	0.31189
	0.6				0.31484
	1				0.32410
1.4	0.6	0.7	0.3	0.3	0.31484
		3			0.29362
		7			0.25200
1.4	0.6	0.7	0	0.3	0.23281
			0.3		0.31484
			0.6		0.08990
1.4	0.6	0.7	0.3	0	0.34768
				0.3	0.31484
				0.6	0.28767

Table 2 contains values of the Nusselt number $-\theta'(0)$, a ratio of convective to conductive heat transfer at the flat plate and normal to its surface, under various conditions. Shear-thinning fluids achieve the highest rate of fluid temperature $\theta(\eta)$ decrease at the surface of the flat plate, followed by Newtonian and shear-thickening fluids. This behavior is consistent with the observed increase in the Nusselt number as the power law index *n* is decreased, when all other parameters are held constant. As expected, an increase in the magnetic parameter *M* or decrease in the Prandtl number *Pr* results in an increase in the Nusselt number. Increasing the velocity slip parameter δ or temperature slip parameter β has the effect of lowering the Nusselt number. Note that as either the velocity or temperature slip parameter is increased toward an infinite slip condition, the temperature of the fluid at the flat plate approaches the bulk fluid temperature, and the Nusselt number approaches zero. The preceding discussion confirms that an increase in the Nusselt number is analogous to an increase in heat transfer and a thinning of the thermal boundary layer.

5. CONCLUSION

In this article, we studied MHD flow and heat transfer of power law fluid over a flat plate with slip boundary conditions, an extension of previous work in the literature. Numerical solutions were calculated using both bvp4c and the shooting method. The agreement observed by direct comparison of the two solutions gives us confidence in our results. We presented velocity and temperature profiles for various physical parameters to highlight the physics of the model and included tables of the associated boundary derivatives.

Generally, we found that increasing the magnetic parameter increases the velocity and decreases the temperature of a power law fluid in the boundary layer. A similar trend in the velocity and temperature profiles is observed as the velocity slip parameter is increased. Increasing the temperature slip parameter results in a decrease in fluid temperature, for a given distance from the flat plate. The fluid velocity is unaffected by variations in the temperature slip parameter. Increasing the Prandtl number results in a decrease in temperature of Newtonian and non-Newtonian fluids, for a given distance from the flat plate.

The basic features of this model may be incorporated in further studies on a variety of flow scenarios in complex media. We anticipate that incorporation of additional features such as multidimensional MHD slip flow and heat transfer of Newtonian and non-Newtonian fluids may follow. We hope that further theoretical and experimental studies may be motivated by our work.

ACKNOWLEDGMENTS

Author JIS would like to acknowledge support from Simons Foundation under grant number 281839.

REFERENCES

Acrivos, A., M. Shah, and E. Petersen (1960). Momentum and heat transfer in laminar boundary-layer flows of non-newtonian fluids past external surfaces. *AIChE Journal 6*(2), pp. 312–317.

Anderson, H. (2002). Slip flow past a stretch-

ing surface. *Acta Mechanica 158*(1), pp. 121–125.

Bhattacharyya, K., S. Mukhopadhyay, and G. Layek (2011). Mhd boundary layer slip flow and heat transfer over a flat plate. *Chinese Physics Letters 28*(2), pp. 024701.

Damseh, R., H. Duwairi, and M. Al-Odat (2006). Similarity analysis of magnetic field and thermal radiation effects on forced convection flow. *Turkish Journal Of Engineering and Environmental Sciences 30*(2), pp. 83–89.

Ghosh, S. and I. Pop (2006). A new approach on mhd natural convection boundary layer flow past a flat plate of finite dimensions. *Heat and Mass Transfer 42*(7), pp. 587–595.

Howell, T., D. Jeng, and K. DeWitt (1997). Momentum and heat transfer on a continuous moving surface in a power law fluid. *International Journal of Heat and Mass Transfer 20*(4), pp. 710–719.

Mahapatra, T., S. Nandy, and A. Gupta (2009). Analytical solution of magnetohydrodynamic stagnation-point flow of a power-law fluid towards a stretching surface. *Applied Mathematics and Computation 215*(5), pp. 1696–1710.

Martin, M. and I. Boyd (2006). Momentum and heat transfer in a laminar boundary layer with slip flow. *Journal of Thermophysics and Heat Transfer 20*(4), pp. 710–719.

Pop, I. and H. Takhar (1983). Thermal convection near a partly insulated vertical flat plate embedded in a saturated porous medium. *Mechanics Research Communications 10*(2), pp. 83–89.

Reddy, B., N. Kishan, and M. Rajasekhar (2012). Mhd boundary layer flow of a non-newtonian power-law fluid on a moving flat plate. *Advances in Applied Science Research 3*(3), pp. 1472–1481.

Schowalter, W. (1960). The application of boundary-layer theory to power-law pseudoplastic fluids: Similar solutions. *AIChE Journal 6*(1), pp. 24–28.